Novel synthesis of medium surface area SiC and their photoluminescence property

YINGJIE LI[a], JIANYING HAO[a,*], XIANJUN LI[b], YINGYONG WANG[c]
[a]*Taiyuan University of Science and Technology, Taiyuan, 030024, PR China*
[b]*Shanxi University, Taiyuan 030013, PR China*
[c]*Institute of Coal Chemistry, Chinese Academy of Sciences, Taiyuan 030001, PR China*

SiC nanoparticles and nanofibers were prepared by simple carbothermal reduction technology. Low-cost water glass and phenolic resin were respectively used as silicon source and carbon source, and cobalt nitrate was added as additive. The synthesized samples were characterized by XRD, FESEM and N_2 adsorption-desorption isotherms. The results show that cobalt catalyst can change the morphology and the surface area of SiC. When molar ratio of cobalt to silicon equal to 0.0025, SiC nanoparticles with average diameter of 30 nm are synthesized and the surface area reach maximum value, 65 m^2g^{-1}. However SiC nanofibers are synthesized with the increase of cobalt content, but the surface area decreases. The synthetic technique has the advantages of simple, efficient and economical. Strong photoluminescence peaks located around 450 nm and 468 nm are observed at room temperature, which can be ascribed to quantum size effects, microstructures and defects within the SiC materials.

(Received January 20, 2016; accepted August 9, 2017)

Keywords: Medium surface area SiC, Carbothermal reduction, Nanoparticles, Nanofibers, Photoluminescence

1. Introduction

Silicon carbide (SiC) nanomaterials have broad applications in ceramic-, metal-, and polymer- matrix composites and abrasive industry owing to their excellent mechanical strength, chemical stability and thermal-shock resistance [1-3]. As a semiconductor material, SiC is suitable for high temperature, high frequency, high power applications [4-6] due to its wide band gap, strong resistance to oxidation and chemical corrosion, high electron drift velocity and high thermal conductivity. These properties make SiC have broad applications in fields of electronic apparatus, irradiance devices and sensors [7-10]. Recently, SiC nanomaterials have also been regarded as a promising catalyst support material [11-13] and photocatalyst [14-15], and showed their superiority in many catalytic reactions. However, the low specific surface area of SiC limits its industrial application. Therefore, there have been various attempts to prepare SiC nanomaterials with high surface areas.

Up to now, high surface area SiC has been prepared by many methods including template synthesis, sol-gel and carbothermal reduction, pyrolysis of polycarbosilane, chemical vapor deposition, thermal evaporation and combustion synthesis. Shi [16] synthesized high surface area SiC (147 m^2g^{-1}) using macroporous carbon as a template. Jin [17] proposed a modified sol-gel method to synthesize SiC with surface area of 112 m^2g^{-1} using phenolic resin and tetraethoxysilane (TEOS) as raw materials. Pol [18] synthesized high surface area SiC (149 m^2g^{-1}) by the pyrolysis of triethylsilane precursor placed in the closed vessel cell filled with inert gas. Gupta [19] prepared SiC powder with high surface area of 97.5 m^2g^{-1} by chemical vapor deposition (CVD). Zhou [20] synthesized SiC nanowires with high surface area of 62 m^2g^{-1} by a simple thermal evaporation technique. Yermekova [21] used silica, magnesium powder and carbon as raw materials and prepared silicon carbide nanopowder with high surface area of 48-104 m^2g^{-1} by combustion synthesis. Most preparation methods exploit expensive carbon or silicon source, complicated apparatus, complex synthesis process and other special conditions (e.g. higher temperature) [22]. These drawbacks may limit the large-scale fabrication of high surface area SiC. Therefore, simple, low-cost preparation of high surface area SiC become particularly important. It has been reported that SiC with a surface area (20-100 m^2g^{-1}) has satisfied the catalytic reaction requirements [23].

Water glass is a common industrial raw material. It is much cheaper and its sources are richer compared with other silicon precursor. Furthermore, when industrial water glass solution is mixed with carbon precursor powder, it can closely coat the surface of the precursor powder and promote the effective contact of C and Si, thereby reduce the reaction temperature of SiC preparation. To the best of our knowledge, the reports on using water glass as raw material to synthesize high surface area SiC were few. Pan [24] synthesized nanocrystalline SiC using the precursor prepared by spray drying slurry of water glass and carbon black. However, the maximum surface area of the synthesized

SiC was much lower (13 m^2g^{-1}).

In this paper, we first report on a simple, efficient, and economical synthesis of medium surface area SiC by carbothermal reduction using low-cost water glass and phenolic resin as raw material and cobalt nitrate as additive. The obtained SiC was characterized by XRD, FESEM and N_2 adsorption-desorption isotherms. Moreover, the photoluminescence (PL) properties of the as-prepared SiC were studied, and strong violet-blue light emission was observed at room temperature.

2. Experimental

Medium surface area SiC was prepared by a simple carbothermal reduction route. First, 16 g of phenolic resin and a certain amount of cobalt nitrate were dissolved in 35 ml of ethanol (AR) under stirring. The ethanol in the solution was naturally volatilized in the fume hood. Second, the C-Co mixture was dried at 80 °C. The dried product was ground into powders, and mixed with 38 ml of water glass (containing 24.73 wt % SiO_2, modulus = 3.33) under stirring. Third, the C-Co-Si mixture was dried at 100 °C for 12 h. The dried mixture was heated in Ar flow (50 mL min-1) to 1000 °C at a rate of 10 °C min^{-1}, then to 1300 °C at a rate of 2 °C min^{-1} and maintained at this temperature for 6 h. After the furnace was cooled down to room temperature, the as-prepared product was heated in air at 700 °C for 3 h to remove residual carbon, and subsequently treated by the mixture of hydrochloric acid (HCl) and hydrofluoric acid (HF) for 48 h to eliminate unreacted silica and other impurities. Finally, a light-green powder was obtained after washing with distilled water and drying.

The above molar ratio of cobalt to silicon ($n_{Co/Si}$) was 0.0025 (marked C1). We adjusted the amount of cobalt nitrate to make $n_{Co/Si}$ reach 0.0051, 0.0112, 0.0175 and 0.0236, and the as-prepared samples were in turn marked as C2, C3, C4 and C5, respectively.

The crystalline phases of the synthesized samples were characterized by X-Ray diffractometer (Philips X'Pert, XRD) using Cu Kα radiation. The sample morphology was examined with S-4800 field emission scanning electron microscope (FESEM). The BET surface area was determined from nitrogen adsorption–desorption isotherms (at 77 K) using a Micromeritics ASAP-2000. The photoluminescence spectra were recorded with a Hitachi, F-7000 fluorescence spectrophotometer at room temperature, using a 370 nm Xe lamp excitation source and 430 nm cut filter.

3. Results and discussion

The formation of SiC precursor is substantially a dehydration reaction between water-soluble water glass and phenolic resin, which can transform the silica sol into the gel. Phenolic resin is acidic solid, while water glass is alkaline sol or viscous substance. For water glass, adjusting its PH value can make the gel formed. Therefore, we added acidic phenolic resin powders to adjust the PH value of water glass, and then the silica gel contained carbon was formed.

Fig. 1 shows the XRD patterns of the synthesized SiC samples. From the patterns, six diffraction peaks are clearly detected. Among these peaks, five strong diffraction peaks can be indexed to cubic β-SiC and the small peak marked with SF is attributed to stacking faults [25]. Besides these peaks, no other crystalline phases such as silica, carbon or other impurities have been detected from the XRD patterns. Moreover, it can be seen that the XRD patterns of the C1-C5 samples are similar, but the diffraction peak intensity of β-SiC are different. It is obvious that the diffraction peak intensity gradually decrease with the increase of molar ratio of cobalt to silicon. When $n_{Co/Si}$ is 0.0025, the diffraction peak intensity of SiC reaches maximum. This indicates that the SiC sample added with this ratio of cobalt nitrate has better crystallinity. When $n_{Co/Si}$ is higher than 0.0025, the diffraction peak intensity of SiC gradually decrease. This phenomenon is mainly because excessive cobalt can be unfavorable for SiC nuclei growth, that is to say, the addition of excessive cobalt can prevent the growth of SiC nuclei.

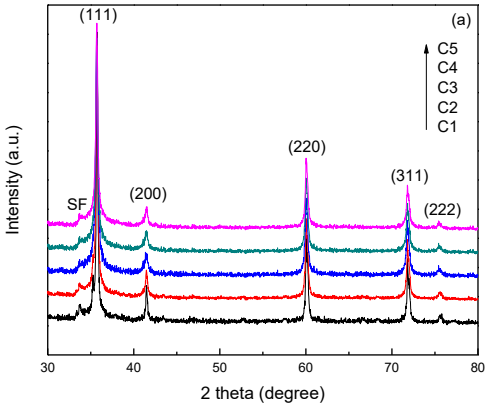

Fig. 1. XRD patterns of the SiC samples: C1-C5 represents the SiC samples with the molar ratio of cobalt to silicon of 0.0025, 0.0051, 0.0112, 0.0175 and 0.0236, respectively

It has been reported that the stacking faults in SiC nanomaterial had a significant effect on their mechanical and thermal properties [25], thus the study of structural defects is particularly important. According to the intensity ratio of the peaks at 33.6° and 41.4° (2θ) ($I_{33.6°}$ / $I_{41.4°}$) [26], the stacking fault densities in these samples were calculated and showed in Fig. 2. It is clear that the stacking fault densities of these samples are all smaller and apparently decrease with the increase of molar ratio of cobalt to silicon. This is because the active phase increases with the addition of cobalt content, which can provide favorable conditions for migration and rearrangement of C and Si in the SiC crystals. This is in agreement with the reported [26]. Moreover, it is well known that the particle size becomes smaller when there are more stacking faults

in the materials. In Fig. 2, the decrease of the stacking fault densities can indicate that the crystallite size of SiC samples can become coarse.

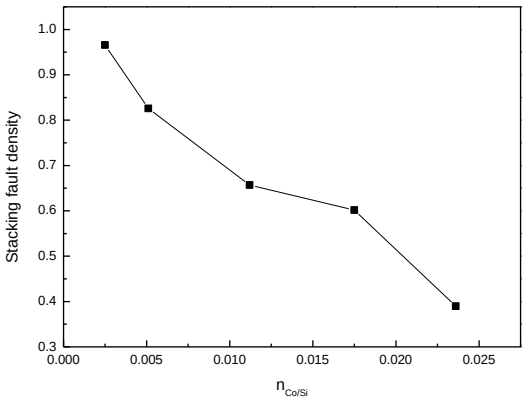

Fig. 2. Influence of the amount of Co catalyst on the stacking faults of SiC

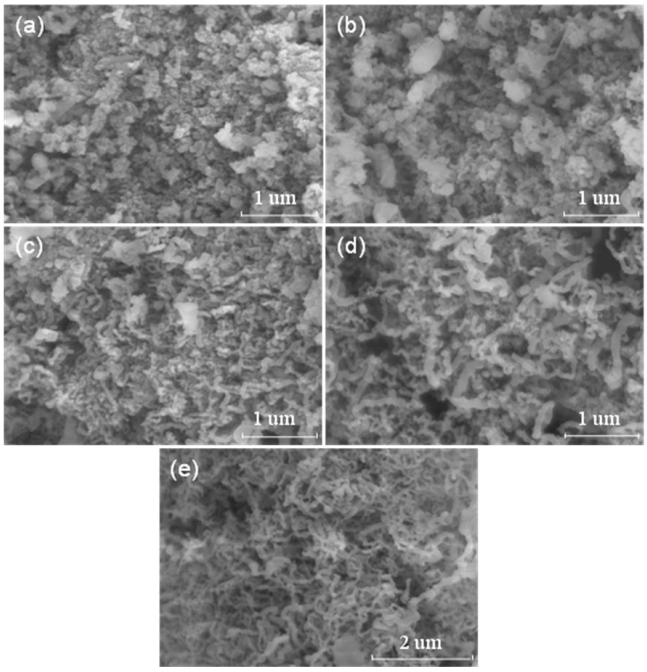

Fig. 3. SEM images of the SiC samples prepared with different amount of Co. $n_{Co/Si}$: (a)-0.0025, (b)-0.0051, (c)-0.0112, (d)-0.0175, (e)-0.0236

Fig. 3 presents SEM images of the SiC products that were prepared by adding different amount of Co, Fig. 3(a)-(e) identify C1-C5, respectively. It can be seen that as $n_{Co/Si}$ equals to 0.0025, the morphology of C1 sample (Fig. 3(a)) is similar granular structure with average diameter of 30 nm. When $n_{Co/Si}$ is up to 0.0051 (Fig. 3(b)), the synthesized SiC particles gradually grow up. Larger particles seen in the figure are caused by the agglomeration of particles. When $n_{Co/Si}$ is up to 0.0112 (Fig. 3(c)), crooked and short SiC nanofibers appear, and the length of SiC nanofibers is less than 1 micron. Thereafter, as $n_{Co/Si}$ continually increases (Fig. 3(d) and 3(e)), crooked and coarse nanofibers of SiC are formed. In the Fig. 3(e), when $n_{Co/Si}$ equals to 0.0236, the length of SiC nanofibers can reach several microns and the diameter of that is between 60 nm and 100 nm. This is in consistent with the analysis result of XRD.

Generally speaking, the morphology and the stacking faults are controlled by the supersaturation of SiO and CO. Generally, the production of the SiC nanostructures consists of two basic steps, the nucleation and growth, respectively [27]. In the experiment, the reduction reaction between SiO_2 and carbon can produce the reductive vapor (CO, SiO). In the nucleation, the carbon atoms on the surface of carbonaceous silica xerogel react with SiO vapor to form SiC embryos and emit CO vapor. However, once the SiC embryos are produced, the reaction of carbon atoms with SiO vapor could be hindered due to the solid diffusion of carbon or the diffusion of SiO vapor molecules through SiC. Then, CO vapor can react with SiO vapor to form SiC crystals, namely the growth of SiC nanofibers. In the process of growth, some liquids can appear owing to the addition of cobalt nitrate, and these liquids accelerate the diffusion of carbon, sequentially improve the reductive reaction C and SiO_2. Therefore, the stacking fault densities of the samples decrease with the increase the amount cobalt nitrate.

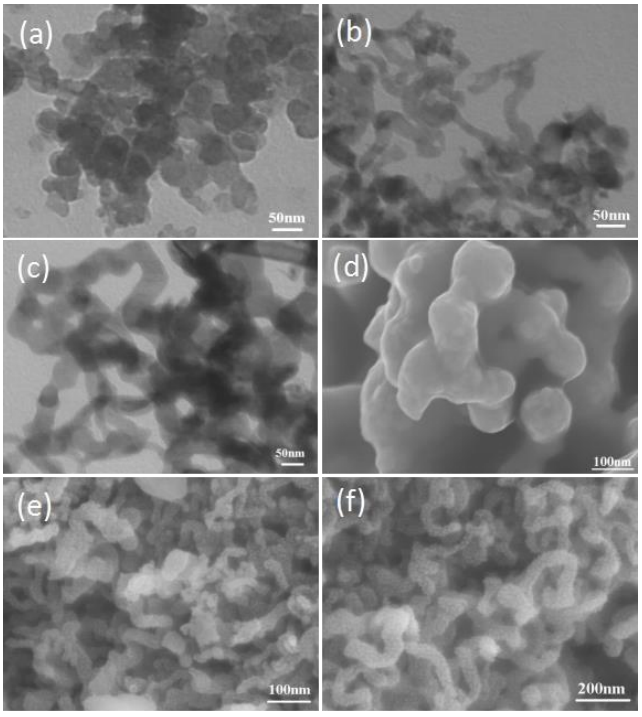

Fig. 4. TEM images of the SiC samples with different $n_{Co/Si}$: (a)-0.0025, (b)-0.0112, (c)-0.0236 and high-magnification SEM images of the SiC samples with different $n_{Co/Si}$: (d)-0.0025, (e)-0.0112, (f)-0.0236

In order to obtain further insight into the morphology of the SiC products, TEM images and high-magnification SEM images are presented in Fig. 4. It is obvious that the agglomeration of SiC particles exist in Fig. 4 (a) and (d). Fig. 4 (b) and (e) show that the surfaces of SiC nanofibers are smooth although the synthesized nanofibers are short. In Fig. 4 (c) and (f), the synthesized SiC nanofibers clearly grow up.

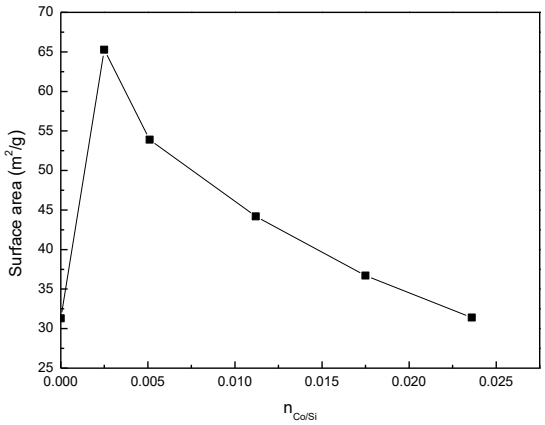

Fig. 5. Dependence of Co content on surface area of SiC

Fig. 5 reveals BET surface areas of the synthesized SiC. It is obvious that surface area of the products gradually decreases with the increase of the molar ratio of cobaltl to silicon. When molar ratio of cobalt to silicon equal to 0.0025, the surface area of synthesized SiC samples reaches maximum, it is 65 m^2g^{-1}. The surface area of the SiC samples gradually decreases with further increase in the cobalt content in the precursor. This is mainly because $n_{Co/Si}$ is greater than 0.0025, the synthesized SiC particles grew up, resulting in the decrease of the surface area. This is consistent with the results of SEM. In addition, when cobalt catalyst was not added in the precursor, the surface area of synthesized SiC is 32 m^2g^{-1}, which is much lower than that of C1 sample. This is because the active phase increases with the addition of cobalt content, which can improve the surface area of SiC.

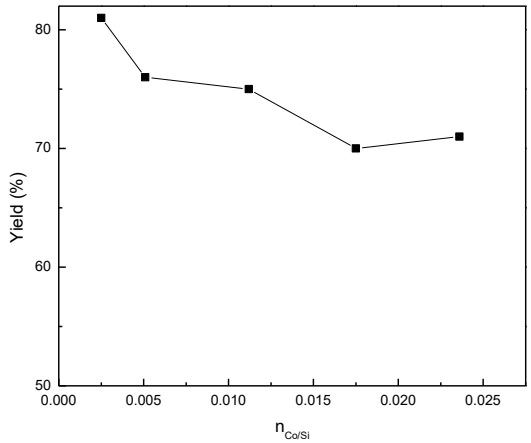

Fig. 6. Effect of $n_{Co/Si}$ on yield of SiC

Fig. 6 shows the yield of the synthesized SiC products. It can be seen that the yield of the synthesized SiC products gradually decrease with the increase of molar ratio of cobalt to silicon, while the yield of all SiC products are above 70%. High yield of SiC nanomaterials is mainly attributed to the complete reaction of carbon and silicon. When $n_{Co/Si}$ is 0.0025, the yield of SiC is as high as 81%. Subsequently the yields gradually decrease with the increase of the molar ratio of cobalt to silicon.

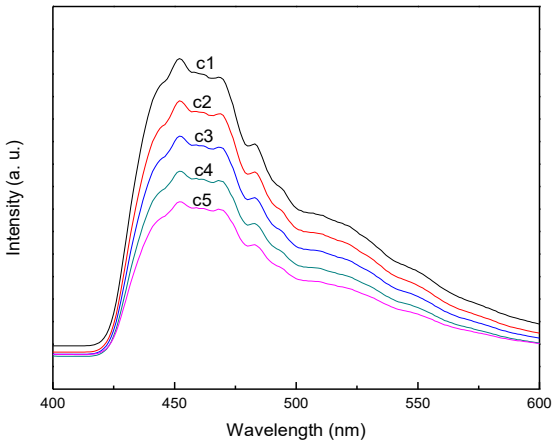

Fig. 7. Room-temperature photoluminescence spectra of the SiC samples

Fig. 7 displays the PL spectra of the as-synthesized SiC under excitation wavelength of 370 nm at room temperature. It is obvious that the overall trend of the PL spectra is very similar, and the PL strength gradually decreases with the increase of molar ratio of cobalt to silicon. The main PL peak is at 450 nm, which is in accordance with the value of the needle-shaped SiC nanowires [28] and SiC nanocrystallites [29] and corresponds to a band gap of 2.76 eV (1240/wavelength = eV) [30]. This peak is generally regarded as the result of the quantum size effects. In addition, it can be clearly observed that there exists another peak at 468 nm (2.65 eV), which was also found in the needle-shaped 3C-SiC nanowires [31]. Chen [31] believed that the strong peak at 468 nm was ascribed to the effect of morphology, orientation, defects and facets' dangling bonds of the needle-shaped nanowires. Compared with the band gap of bulk 3C-SiC (2.23 eV), the PL spectra here are all considerably blue-shifted. In the spectra, there exists a similar shoulder between 456 nm and 465 nm, which may be the result of microstructures and defects within the nanoparticles and nanofibers. Due to its intensive blue-green light emission, SiC nanofibers may have potential application in light emitting diodes, field electron emission and display devices especially for the environment of high temperature and high irradiation.

4. Conclusion

Medium surface area SiC was successfully synthesized by simple carbothermal reduction of a mixture of phenolic resin and water glass with cobalt catalyst. SiC nanoparticles are prepared as the molar ratio of cobalt to silicon is 0.0025, while SiC nanofibers are obtained as the molar ratio of cobalt to silicon is higher than 0.0025. When the molar ratio of cobalt to silicon is 0.0025, the synthesized SiC nanoparticles have better crystallinity and the surface area also reaches maximum value (65 m^2g^{-1}), which can meet the industrial requirements. When the molar ratio of cobalt to silicon is 0.0236, the synthesized SiC nanofibers have the length of several microns and the average diameter of 90 nm. The prepared SiC nanoparticles and nanofibers have high yield. There are stable and intensive PL peaks along 450 nm and 468 nm under excitation wavelength of 370 nm at room temperature, which has considerable blue shifts relative to the bulk 3C-SiC. The SiC preparation technology, using economic raw materials and simple process, will be feasible for future industrial production.

Acknowledgements

The financial support of the School Doctoral Program Foundation (grant no. 20132007) is gratefully acknowledged.

References

[1] J. J. Chen, Y. Pan, W. H. Tang, Q. Shi, Nano-Micro Lett. **2**(1), 11 (2010).
[2] K. B. Nie, X. J. Wang, X. S. Hu, L. Xu, K. Wu, M. Y. Zheng, Mater. Sci. Eng. A **528**(15), 5278 (2011).
[3] S. Meng, G Q. Jin, Y. Y. Wang, X. Y. Guo, Mater. Sci. Eng. A **527**(21-22), 5761 (2010).
[4] W. M. Zhou, X. Liu, Y. F. Zhang, Appl. Phys. Lett. **89**(22), 223124 (2006).
[5] J. J. Chen, J. D. Zhang, M. M. Wang, L. Gao, Y. Li, J. Alloys Compd. **605**, 168 (2014).
[6] J. J. Chen, X. Liao, M. M. Wang, Z. X. Liu, J. D. Zhang, L. J. Ding, L. Gao, Y. Li, Nanoscale **7**(14), 6374 (2015).
[7] H. K. Seong, H. J. Choi, S. K. Lee, J. I. Lee, D. J. Choi, Appl. Phys. Lett. **85**(7), 1256 (2004).
[8] L. G Zhang, W. Y. Yang, J. Hua, Z. H. Zheng, Z. P. Xie, H. Z. Miao, L. An, Appl. Phys. Lett. **89**(14), 143101 (2006).
[9] D. L. Zhao, F. Luo, W. C. Zhou, J. Alloys Compd. **490**(1-2), 190 (2010).
[10] J. J. Chen, Q. Shi, L. P. Xin, Y. Liu, W. H. Tang, Curr. Nanosci. **8**(2), 226 (2012).
[11] X. N. Guo, R. J. Shang, D. H. Wang, G Q. Jin, X. Y. Guo, K. N. Tu, Nanoscale Res. Lett. **5**, 332 (2010).
[12] N. Keller, C. Pham-Huu, M. J. Ledoux, Appl. Catal. A **217**(1-2), 205 (2001).
[13] G J. Zhi, X. N. Guo, Y. Y. Wang, G Q. Jin, X. Y. Guo, Catal. Commun. **16**(1), 56 (2011).
[14] N. A. Kouame, D. Robert, V. Keller, N. Keller, C. Pham, P. Nguyen, Catal. Today **161**(1), 3 (2011).
[15] J. Y. Hao, Y. Y. Wang, X. L. Tong, G Q. Jin, X. Y. Guo, Int. J. Hydrogen Energy **37**, 150384 (2012).
[16] Z. C. Liu, W. H. Shen, W. B. Bu, H. R. Chen, Z. L. Hua, L. X. Zhang, L. Li, J. L. Shi, S. H. Tan, Microporous Mesoporous Mater. **82**(1-2), 137 (2005).
[17] G Q. Jin, X. Y. Guo, Microporous Mesoporous Mater. **60**(1-3), 207 (2003).
[18] V. G Pol, S. V. Pol, A. Gedanken, Chem. Mater. **17**(7), 1797 (2005).
[19] A. Gupta, T. Ghosh, C. Jacob, J. Mater. Sci. **42**(13), 5142 (2007).
[20] W. M. Zhou, L. J. Yan, Y. Wang, Y. F. Zhang, Appl. Phys. Lett. **89**(1), 013105 (2006).
[21] Z. Yermekova, Z. Mansurov, A. Mukasyan, Ceram. Int. **36**(8), 2297 (2010).
[22] J. J. Chen, Q. Shi, L. P. Xin, Y. Liu, R. J. Liu, X. Y. Zhu, J. Alloys Compd. **509**(24), 6844 (2011).
[23] J. Parmentier, J. Patarin, J. Dentzer, C. Vix-Guterl, Ceram. Int. **28**(1), 1 (2002).
[24] S. L. Pan, J. J. Zhang, Y. F. Yang, G Z. Song, Ceram. Int. **34**(2), 391 (2008).
[25] W. S. Seo, K. Koumoto, S. Aria, J. Am. Ceram. Soc. **83**(10), 2584 (2000).
[26] W. S. Seo, K. Koumoto, S. Arai, J. Am. Ceram. Soc. **81**(5), 1255 (1998).
[27] L. P. Xin, Q. Shi, J. J. Chen, W. H. Tang, N. Y. Wang, Y. Liu, Y. X. Lin, Mater. Charact. **65**, 55 (2012).
[28] V. G. Pol, S. V. Pol, A. Gedanken, S. H. Lim, Z. Zhong, J. Lin, J. Phys. Chem. B **110** (23), 11237 (2006).
[29] J. Y. Fan, X. L. Wu, R. Kong, T. Qiu, G S. Huang, Appl. Phys. Lett. **86**(17), 171903 (2005).
[30] J. J. Chen, W. H. Tang, L. P. Xin, Q. Shi, Appl. Phys. A **102**(1), 213 (2011).
[31] J. J. Chen, R. B. Wu, G. Y. Yang, Y. Pan, J. Lin, L. L. Wu, R. Zhai, J. Alloys Compd. **456**(1-2), 320 (2008).

*Corresponding author: jyty2280@163.com